

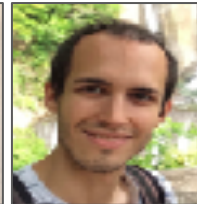
A review of numerical techniques to simulate seismic cycles



2022 Seismic Cycle Symposium ● 17-19 October 2022



K. Allison, S. Barbot, A. Gabriel, L. Hwang, D. May, P. Romanet,
P. Segall, L. Dal Zilio





Seismic Cycle Working Group

Goals

- Build a community of modelers and developers focused on the specific challenges of modeling seismic cycles.
- Develop and promote well documented, open-source software for seismic cycle modeling based on a variety of numerical methods that inter-operate.

Timeline

- May-July 2022: Weekly online seminar. YouTube playlist: <https://www.youtube.com/playlist?list=PLdy04DoEepEwTtFOR7MkQX1VlpMDOXLE9>
- October 17-19, 2022: Online symposium <https://geodynamics.org/events/details/276>
- December 2022: Whitepaper and strategic plan for community engagement and code development plan.
- 2023: Implementation of strategic plan and engaging community in the development and publication of software

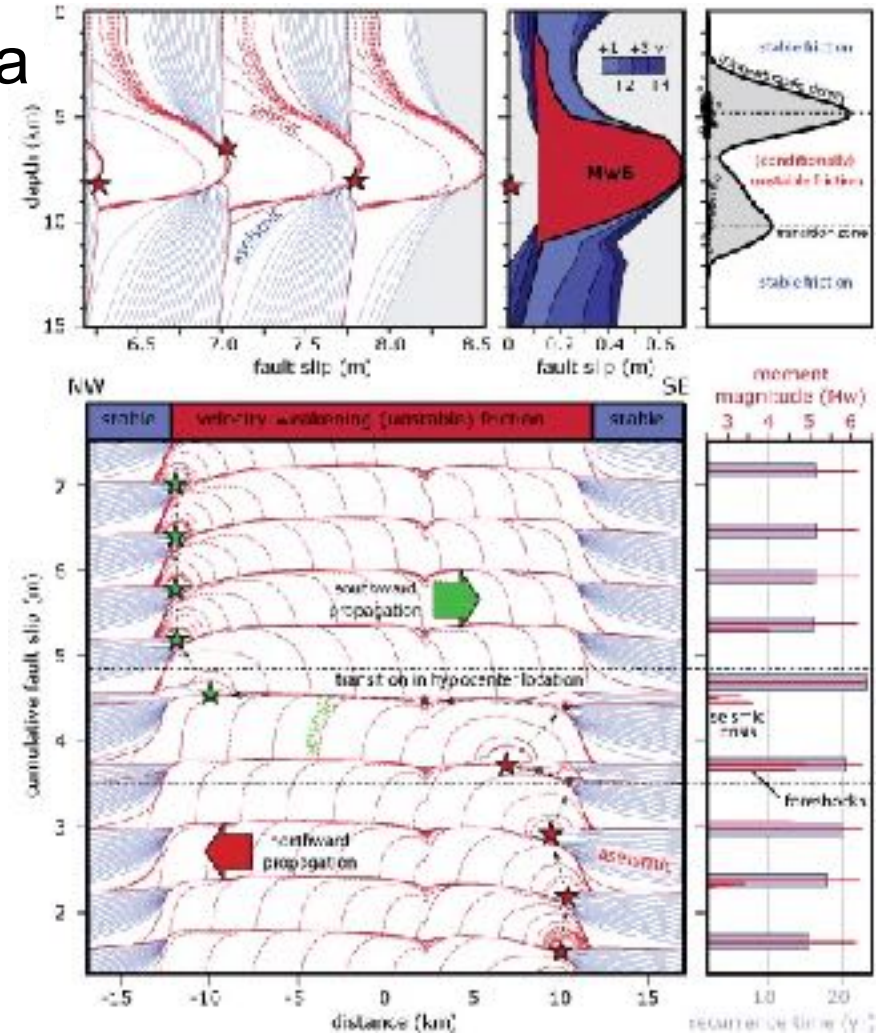
Motivations

Modeling of seismo-geodetic data

Seismic cycle simulations connect seismicological, geodetic, and geological observations through a physical representation of the lithosphere.

Simulations highlight controlling processes and test scientific questions (hypothesis testing).

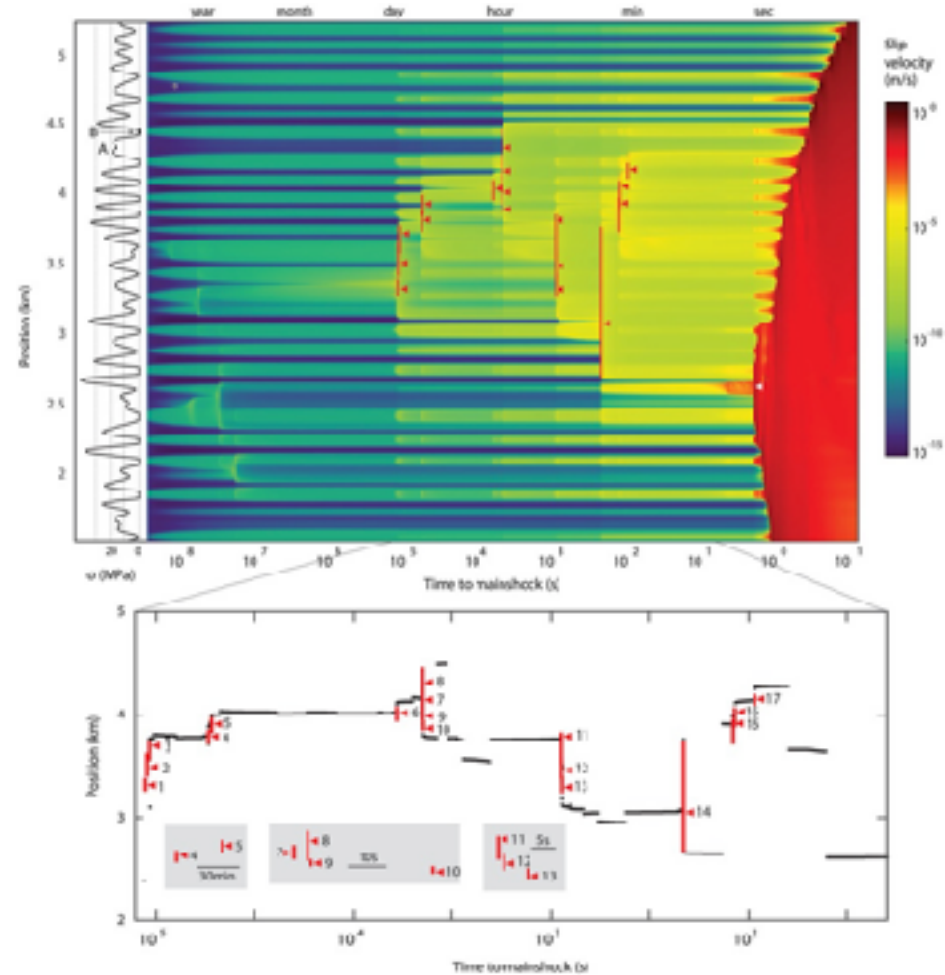
Example: Cycle of Mw 6.0 earthquakes on the San Andreas Fault at Parkfield, CA demonstrating the change of hypocenter location, as observed between 1996 and 2004 events (*Barbot et al. 2012*).



Beyond observations

Seismic cycle simulations facilitate the inspection of phenomena or physical quantities that cannot be observed directly.

Example: clustering of foreshocks accompanying the nucleation of large earthquakes. The spatial variations of normal stress associated with a rough fault allow the nucleation of tiny earthquakes in the acceleration phase of a macroscopic nucleation (*Cattania & Segall 2021*).



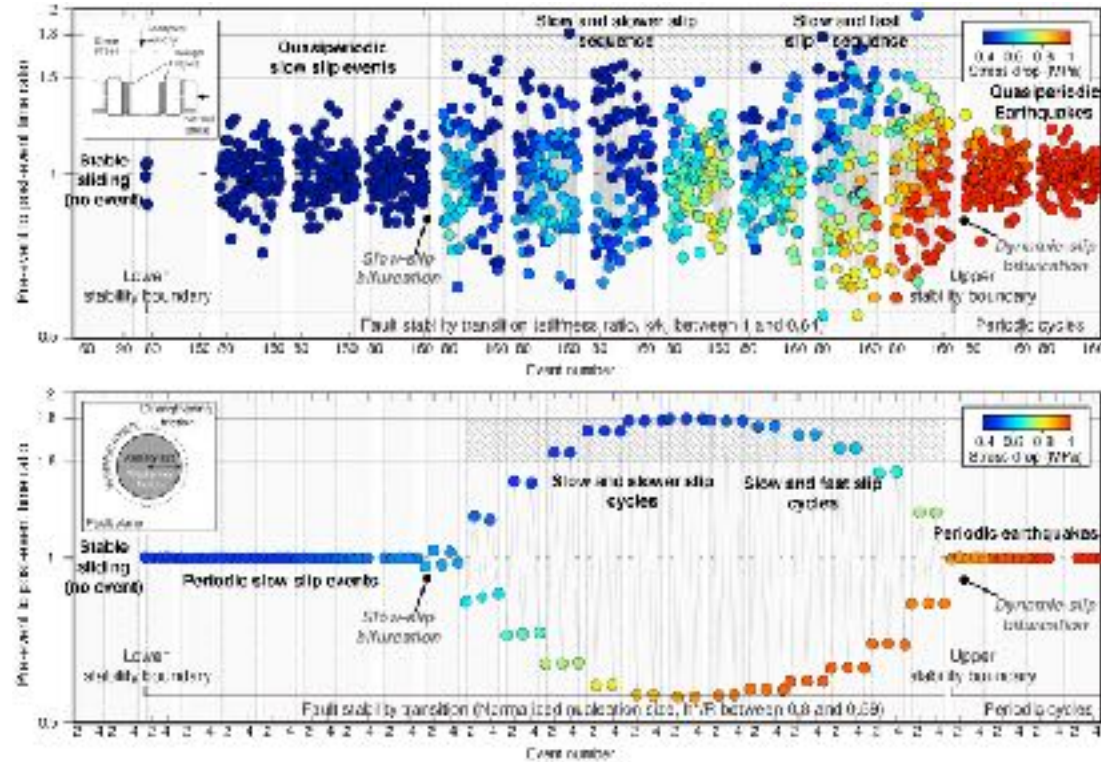
(*Cattania & Segall 2021*)

Prediction of rupture styles

Seismic cycle simulations illustrate how theory may explain observations in nature.

In some occasions, some phenomena are predicted in silico, and verified in the laboratory.

Example: Bifurcation of recurrence patterns and rupture styles around the stability transition predicted by *Veedu & Barbot (2016)* subsequently observed in the laboratory (*Veedu et al. 2020*).



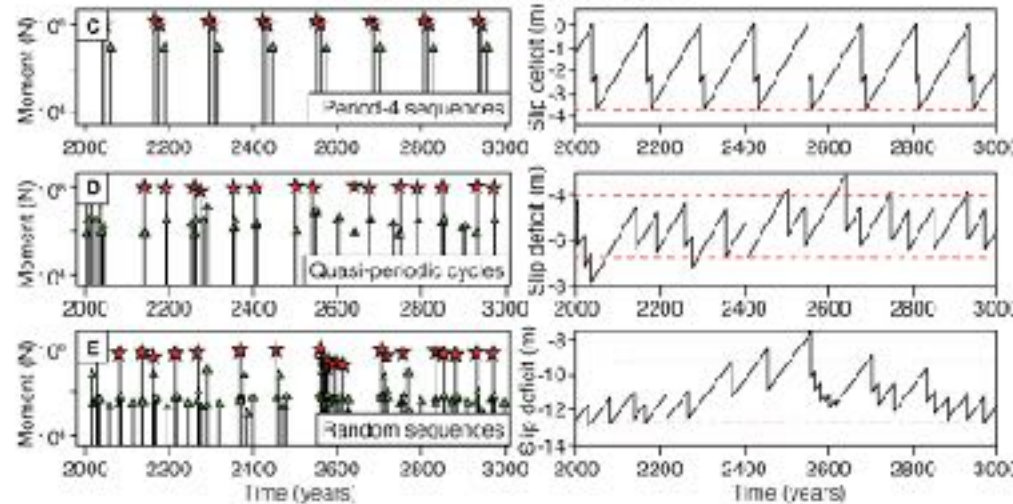
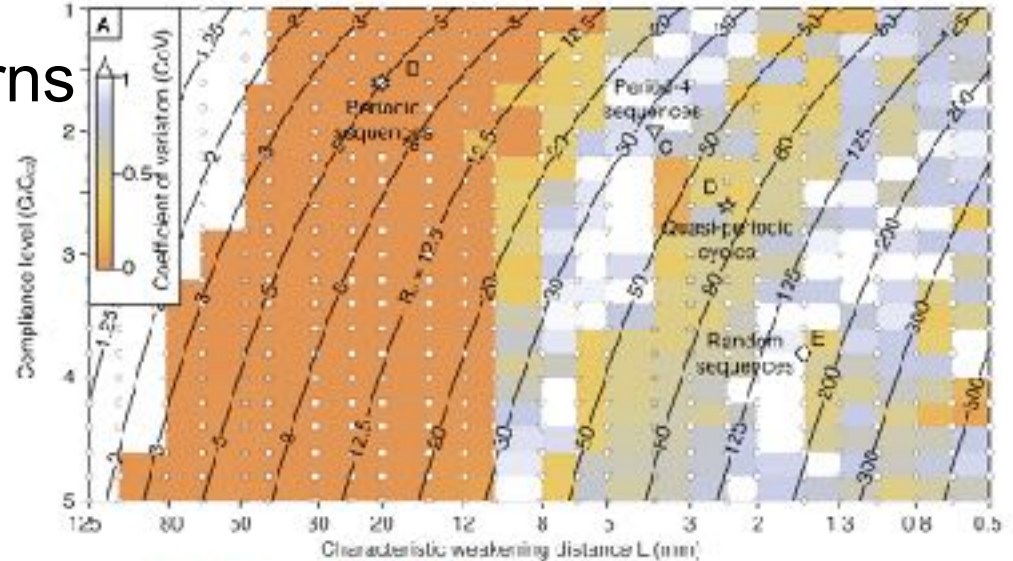
(*Veedu et al. 2020*)

Controls on recurrence patterns

Seismic cycle simulations predict the style and recurrence patterns of frictional instabilities based on physical parameters.

Place natural observations in a physical context.

Example: transition from single-periodic to chaotic cycles and from crack-like to pulse-like ruptures with reduction of the characteristic nucleation size (*Nie & Barbot, 2022*)



Governing equations

Elasticity

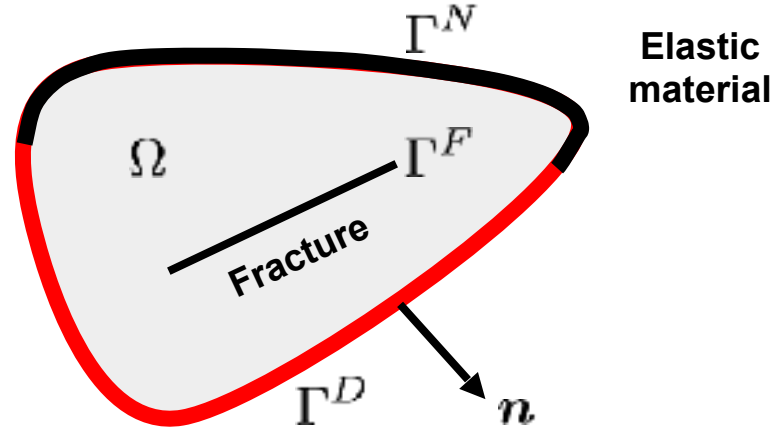
Elastic deformation of solids results from quasi-equilibrium between attractive and repulsive forces at the atomic level. Elastic deformation is reversible and measured from an equilibrium configuration. The conservation of **linear momentum** provides the elasto-dynamic equation

$$\nabla \cdot \boldsymbol{\sigma} + \mathbf{f} = \rho \ddot{\mathbf{u}}$$

in the volume Ω , subject to boundary conditions constraining displacement or traction. Conservation of **angular momentum** provides

$$\boldsymbol{\sigma} = \boldsymbol{\sigma}^t$$

Faults are internal **dislocations** associated with addition conditions on relative displacement (slip) or its velocity. Seismic cycle models typically implement a friction law that balances stress, state, and the velocity of sliding.



$$\mathbf{u} = \mathbf{g}^D \quad \text{on } \Gamma^D \quad (\text{displacement})$$

$$\boldsymbol{\sigma} \cdot \mathbf{n} = \mathbf{g}^N \quad \text{on } \Gamma^N \quad (\text{traction})$$

$$[[\mathbf{u}]] = \mathbf{g}^F \quad \text{on } \Gamma^F \quad (\text{slip})$$

$$\mathbf{u}|_{t=0} = \mathbf{u}_0(\mathbf{x}) \quad \text{initial conditions}$$

$$\frac{\partial \mathbf{u}}{\partial t} |_{t=0} = \mathbf{v}_0(\mathbf{x})$$

Elasto-static equilibrium

Seismic cycles modeling can be simulated with or without the radiation of seismic waves.

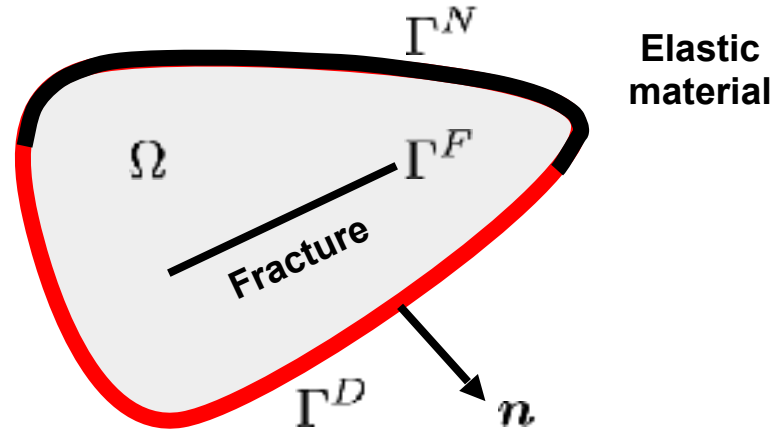
Under the **quasi-dynamic approximation**, the elasto-static equilibrium is considered

$$\nabla \cdot \boldsymbol{\sigma} + \mathbf{f} = \mathbf{0}$$

and the time dependence emerges from the friction law.

Ignoring seismic waves leads to reduction of rupture propagation speed and differences in rupture styles. For example, super-shear ruptures are not possible.

Solving the elasto-static or the elasto-dynamic equations require different numerical methods. The elasto-dynamic equation is **hyperbolic** and can be solved efficiently with the finite difference method. The elasto-static equation is **elliptic** and can be solved efficiently with Fourier transforms or Green's functions.



$$\mathbf{u} = \mathbf{g}^D \quad \text{on } \Gamma^D \quad (\text{displacement})$$

$$\boldsymbol{\sigma} \cdot \mathbf{n} = \mathbf{g}^N \quad \text{on } \Gamma^N \quad (\text{traction})$$

$$[[\mathbf{u}]] = \mathbf{g}^F \quad \text{on } \Gamma^F \quad (\text{slip})$$

$$\mathbf{u}|_{t=0} = \mathbf{u}_0(\mathbf{x}) \quad \text{initial conditions}$$

$$\frac{\partial \mathbf{u}}{\partial t} |_{t=0} = \mathbf{v}_0(\mathbf{x})$$

Friction

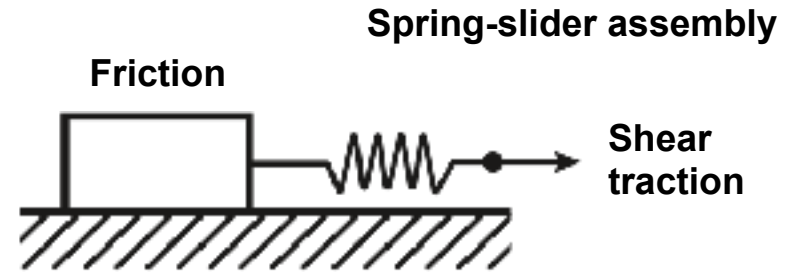
Friction refers to the force resisting sliding between two solids, even separated by a thin gouge layer (Byerlee 1978).

The behavior of a fault representative element is often described by a **spring-slider assembly**, whereby the slider resists the shear traction.

The localized deformation within the fault zone can be described as an internal strain-rate or as the velocity of relative motion. The constitutive behavior can be written as a power-law

$$V = V_0 \left(\frac{\tau}{\mu_0 \bar{\sigma}} \right)^n \left(\frac{d}{d_0} \right)^{-m} \exp \left[- \frac{Q}{RT} \right]$$

involving a state variable that captures the time-dependent healing and weakening resulting from structural evolution within the fault zone.



The aging of the fault zone and its rejuvenation during sliding can be captured by an evolution law

$$\frac{\dot{d}}{d} = \frac{G}{pd^p} \exp \left[- \frac{H}{RT} \right] - \frac{\lambda V}{2h}$$

For modeling of three-dimensional deformation, the constitutive law must be written in vector form:

$$\mathbf{V} = V_0 \left(\frac{\tau}{\mu_0 \bar{\sigma}} \right)^{n-1} \left(\frac{d}{d_0} \right)^{-m} \exp \left[- \frac{Q}{RT} \right] \frac{\mathbf{t}}{\mu_0 \bar{\sigma}}$$

Modeling earthquakes requires additional weakening mechanisms, such as **flash weakening** or **thermal pressurization**. Many friction and evolution laws exist.

Viscoelasticity

Viscoelasticity refers to the time-dependent accumulation of **plastic strain** in the country rocks by diffusion creep, dislocation creep, or other micro-physical mechanisms (Karato & Wu 1993).

Viscoelastic flow is often represented by a **spring-dashpot assembly**. For example, the constitutive law controlling steady-state creep can be described by a **Maxwell body**, expressed in terms of some stress and strain-rate tensors invariants

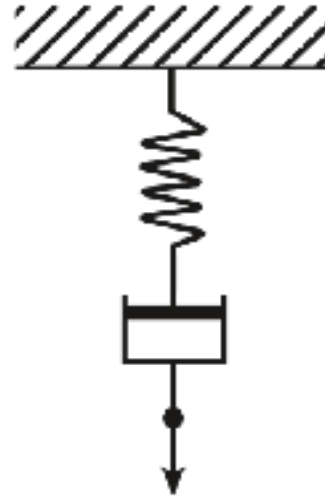
$$\dot{\gamma} = A \tau^n$$

For seismic cycle modeling, a constitutive law must be written in tensor form

$$\dot{\epsilon}^i = A \tau^{n-1} \sigma^i$$

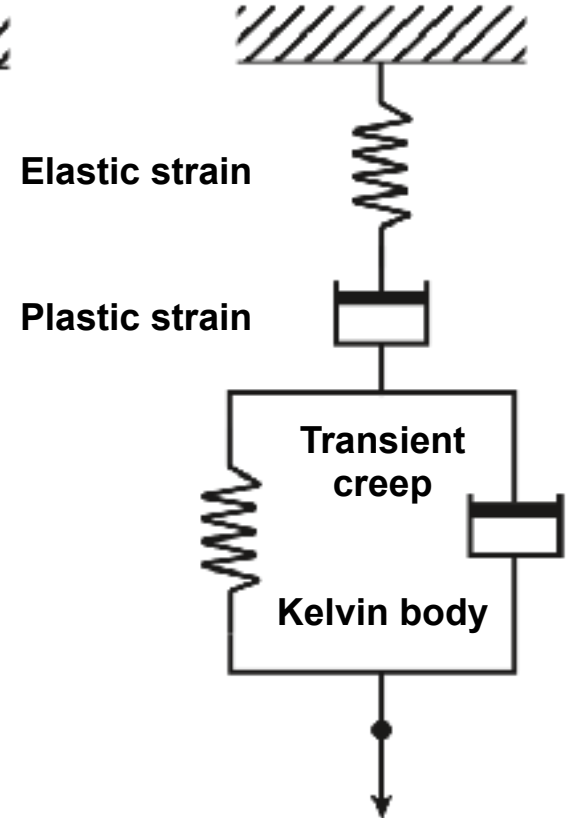
Transient creep can be described with a **Burgers assembly**.

Maxwell assembly



Deviatoric stress

Burgers assembly



Elastic strain

Plastic strain

Transient creep

Kelvin body

Deviatoric stress

Viscoelasticity

The governing equations can be derived by separating the **total strain tensor** into the **elastic** and **anelastic components**

$$\dot{\boldsymbol{\epsilon}} = \dot{\boldsymbol{\epsilon}}^i + \dot{\boldsymbol{\epsilon}}^e$$

Noticing that stress is only a function of the elastic strain, conservation of linear momentum provides

$$\nabla \cdot (\mathbf{C} : \dot{\boldsymbol{\epsilon}}) + \dot{\mathbf{f}} = \mathbf{0}$$

where the equivalent body force is (Barbot et al. 2010)

$$\dot{\mathbf{f}} = -\nabla \cdot (\mathbf{C} : \dot{\boldsymbol{\epsilon}}^i)$$

Finally, we complete the description with a **constitutive law** of the form

$$\dot{\boldsymbol{\epsilon}}^i = \dot{\boldsymbol{\epsilon}}^i(\boldsymbol{\sigma}, T, \dots) = \dot{\gamma} \mathbf{R}$$

For example, diffusion creep follows the relation

$$\dot{\boldsymbol{\epsilon}}^i = \frac{\boldsymbol{\sigma}'}{\eta}$$

For dislocation creep, the effective viscosity depends on stress

$$\dot{\boldsymbol{\epsilon}}^i = A \sigma^{n-1} \exp\left[-\frac{Q + p\Omega}{RT}\right] \boldsymbol{\sigma}'$$

Transient creep and steady-state creep can be modeled with a state variable (Masuti et al. 2016; Masuti & Barbot, 2021).

Poroelasticity

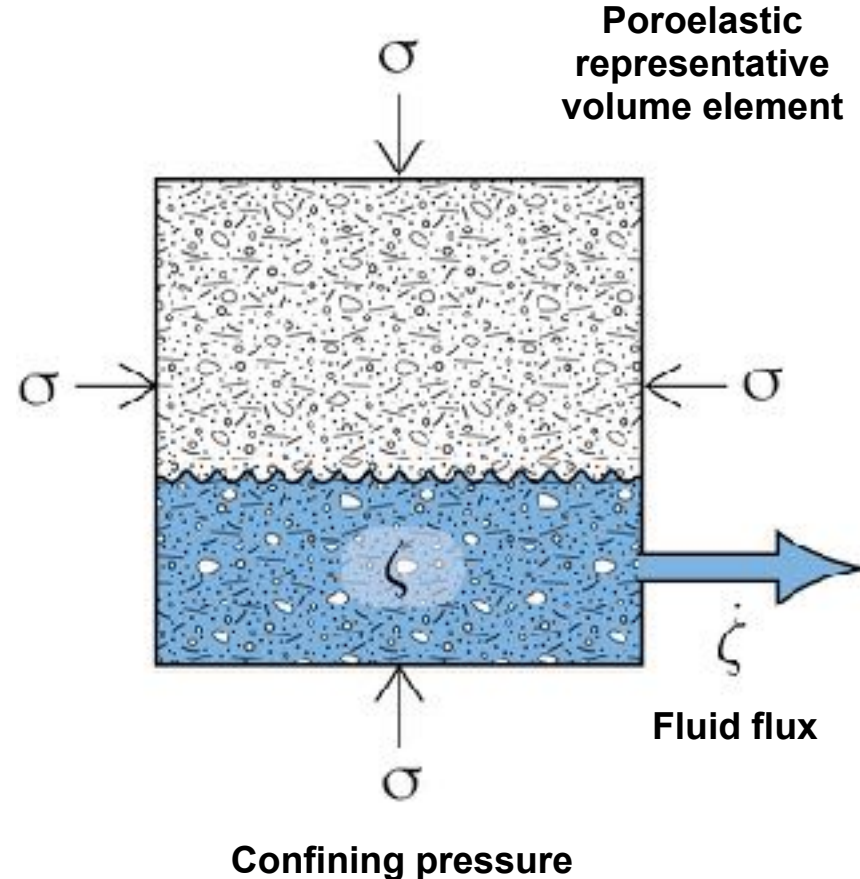
In a **poroelastic material**, a representative volume element consists of a solid matrix (skeleton) and a fluid-saturated connected pore space. The elastic response is different in **undrained** and **drained conditions**.

The movement of fluids in the pore space is coupled with the solid deformation. The instantaneous response can be described by

$$\nabla \cdot (\mathbf{C}_u : \dot{\boldsymbol{\epsilon}}) - K_u B \nabla \dot{\zeta} = \rho \ddot{\mathbf{u}}$$

The fluids are forced to migrate through the pore space following **Darcy flow**, where pore pressure depends on fluid content and strain of the skeleton

$$\dot{\zeta} = D \nabla^2 \left[(1 - \beta) \zeta - \alpha \frac{\sigma}{K_u} \right]$$



Panorama of techniques

Panorama of modeling techniques

** indicates open-source codes available*

Boundary integral method (BIM)

- 1) Fully-dynamic boundary integral method (BIM-fd)
- 2) Fully-dynamic spectral boundary integral method (SBIM-fd)
- 3) Quasi-dynamic boundary integral method (BIM-qd) *
- 4) Quasi-dynamic spectral boundary integral method (SBIM-qd) *
- 5) Quasi-dynamic integral method (IM-qd)

Volumetric methods

- 1) Finite difference method (FD) *
- 2) Continuous Galerkin Finite element method (CG-FEM) *
- 3) Discontinuous Galerkin Finite element method (DG-FEM) *

Hybrid methods

Method 1: Fully-dynamic boundary integral method (BIM)

For dislocations embedded in an elastic material, the displacement is a linear function of fault slip, called a **Green's function**. The displacement field can be calculated using the integral equation

$$\mathbf{u}(\mathbf{x}, t) = \int_0^\infty \iint_{\partial\Omega} \mathbf{C} : (\mathbf{s} \otimes \mathbf{n} \otimes \nabla \mathbf{G}(\mathbf{x}, t, \mathbf{y}, t')) \, dA(\mathbf{y}) dt'$$

The Green's functions for elasto-dynamics are available in **closed form** for a homogeneous elastic full space. For example, in the case of a slip distribution on a planar fault in mode III, the stress distribution is given by

$$\tau(\mathbf{x}, t) = - \int_0^t \int_{\partial\Omega} \frac{G}{2\pi\beta^2} \frac{s}{\left((t - \tau)^2 - \frac{(x_1 - y_1)^2}{\beta^2} \right)^{3/2}} \mathcal{H} \left(t - \tau - \frac{|x_1 - y_1|}{\beta} \right) \, dy d\tau$$

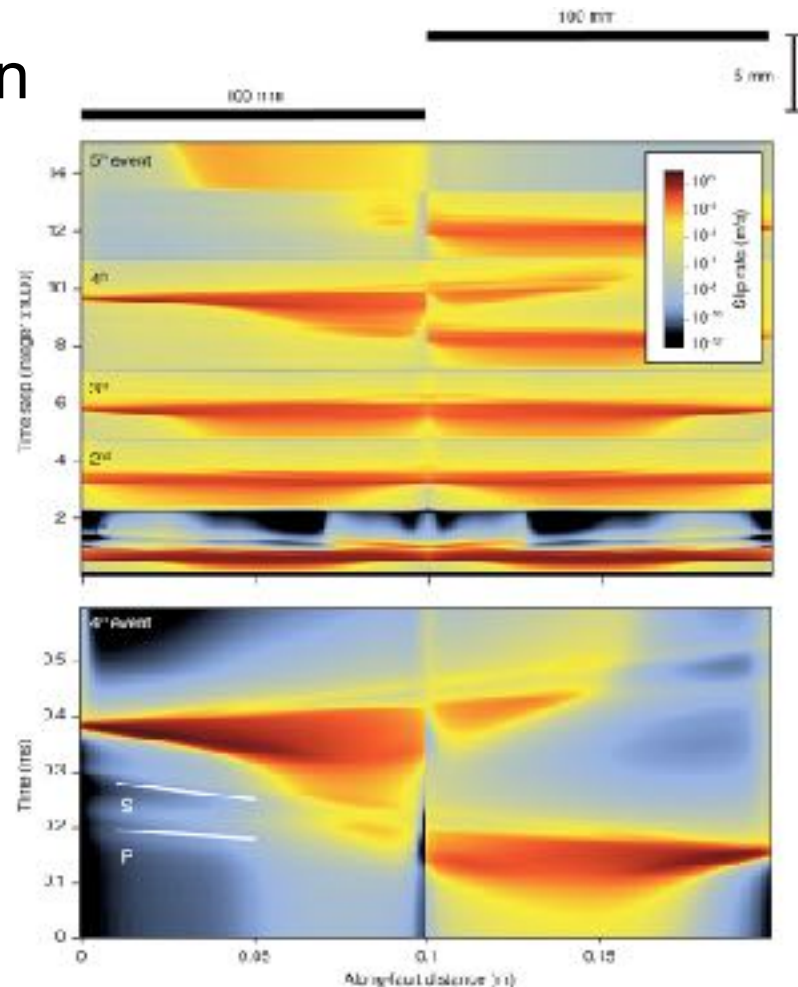
The **boundary integral method** (BIM) uses such analytic solutions to represent the elastic interactions. As a result, only the fault plane must be discretized numerically, largely reducing the numerical cost. The integral equation can be approximated by a finite sum using the trapezoidal rule, reducing the computation to a small number of matrix-vector multiplications.

Application of BIEM-fd in plane-strain

Using the boundary integral method and calculating stress interactions with space-time Green's function is computationally intensive, but versatile.

Example: Cycle of ruptures across a step-over at the laboratory scale in two-dimensional plane-strain condition (*Baoning Wu, pers. comm. 2022*). The seismic waves radiated across the step-over, modulating normal and shear stress.

Using the same approach for three-dimensional simulations is computationally prohibitive without modification.



(*Baoning Wu, pers. comm. 2022*)

Method 2: Fully-dynamic spectral boundary integral method (SBIM-fd)

As the stress interaction represents a convolution, it can be computed efficiently using the convolution theorem and the Fast Fourier transform (FFT). In mode II, the fully-dynamic stress interaction can be written

$$\tau(k, t) = \underbrace{-\mu|k| \left(1 - \frac{\beta^2}{\alpha^2}\right) s(k, t)}_{\text{Static term}} - \underbrace{\mu|k| \int_0^t C_{II}^T(k, \tau) \dot{s}(k, t - \tau) d\tau}_{\text{Dynamic term}},$$

where

$$\begin{aligned} C_{II}^T(k, t) = & \left(\beta^2 k^2 t^2 + \frac{\beta^2}{\alpha^2} \right) W(\alpha kt) - (\beta^2 k^2 t^2 + 1) W(\beta kt) \\ & - \frac{\beta^2}{\alpha^2} J_1(\alpha kt) + \frac{1}{2} J_1(\beta kt) \\ & - \frac{\beta^2}{\alpha} kt J_0(\alpha kt) + \beta kt J_0(\beta kt). \end{aligned}$$

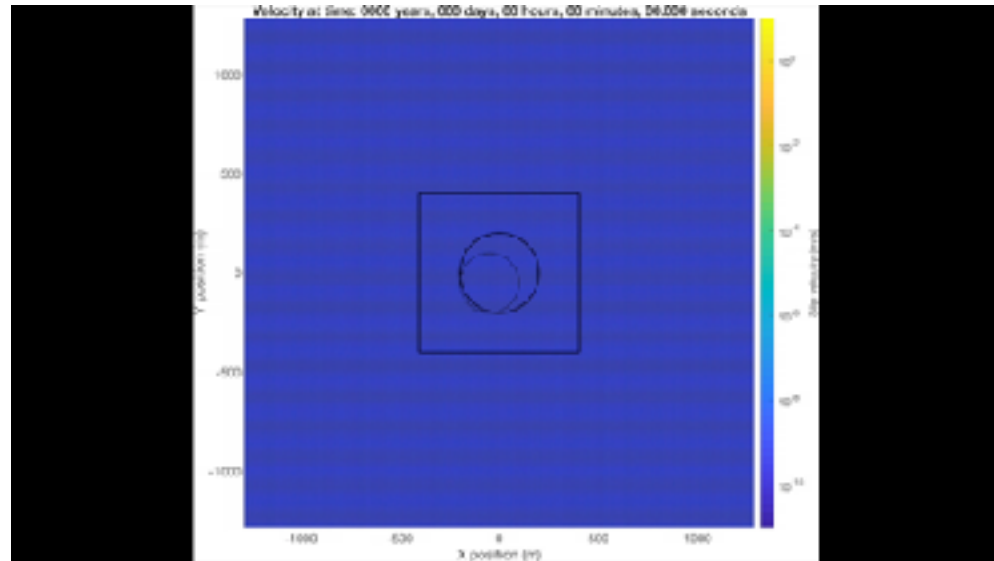
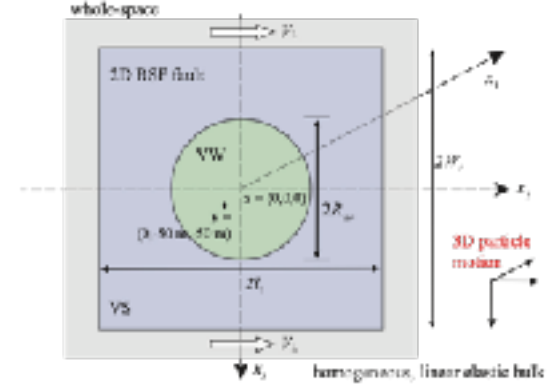
The FFT reduces the computational cost to $N^2 \log(N)$, where N is the number of samples on the fault.

Applications of SBIM-fd with FastCycles

In practice, the spectral boundary integral method (SBIEM) is the most computationally efficient method to simulate seismic cycles.

Example: The SCEC sequence of earthquake and aseismic slip (SEAS) benchmark BP7 (https://strike.scec.org/cvws/seas/benchmark_descriptions.html), computed using FastCycles (*P. Romanet, pers. comm. 2022*)

Fully-dynamic simulation of circular patch (SCEC SEAS benchmark BP7-fd)



Method 3: Quasi-dynamic boundary integral method (BIM-qd)

The boundary integral method can be used within the **quasi-dynamic approximation**, whereby the elastic interactions are limited to the static component combined with the instantaneous effect of fault slip called radiation damping. The stress interaction can be written

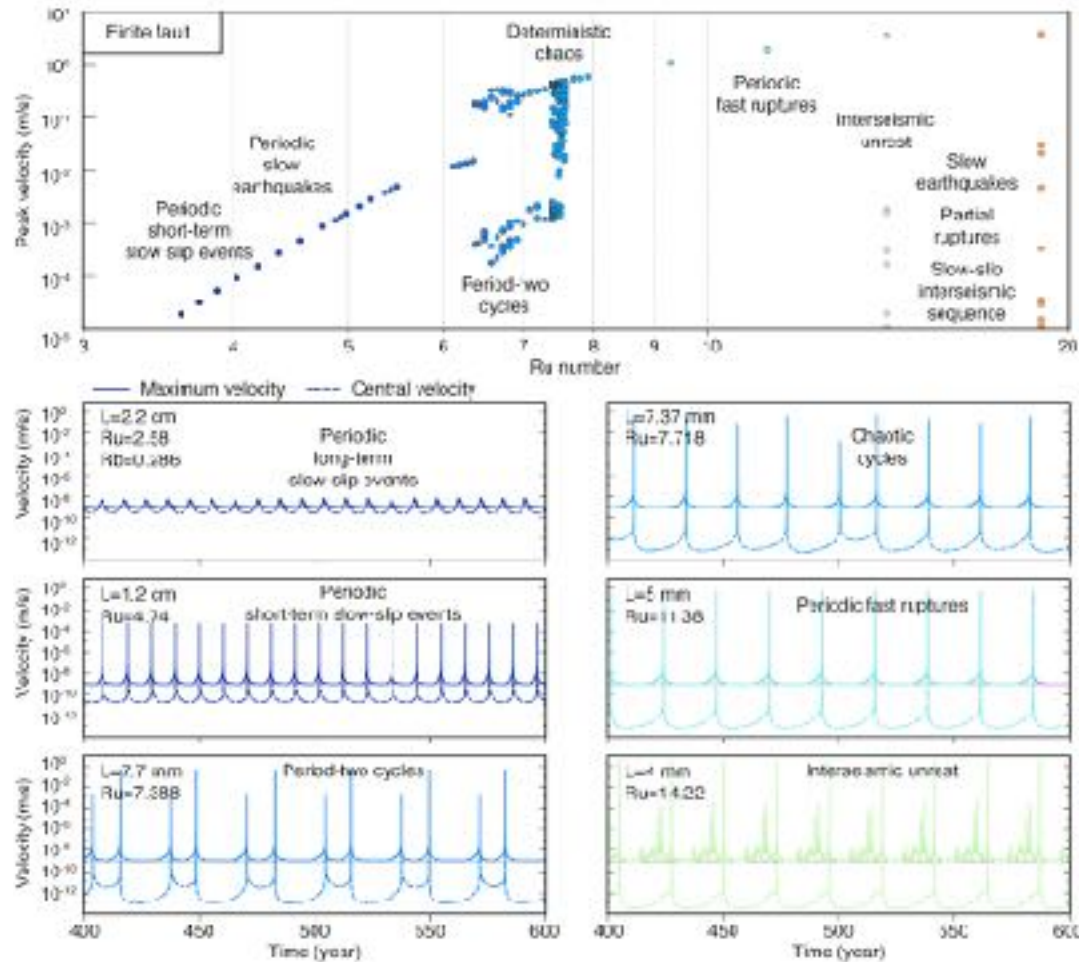
$$\tau(\mathbf{x}, t) = \underbrace{-\frac{G}{\pi} \left(1 - \frac{\beta^2}{\alpha^2}\right) \int_{\partial\Omega} \frac{1}{x-y} \frac{d}{dy} [s(y, t)] dy}_{\text{Static term}} \quad \underbrace{-\frac{G}{2\beta} \dot{s}(y, t)}_{\text{Radiation damping term}}$$

The quasi-dynamic approximation dramatically alleviates the computational cost.

Application of BIM-*qd* with Unicycle

The quasi-dynamic boundary integral method is efficient and versatile in two-dimensional models, but three-dimensional deformation is computationally expensive ($\sim N^2$).

Example: Use numerical simulations to explore physical variables controlling rupture style and recurrence patterns (*Barbot, 2019*).



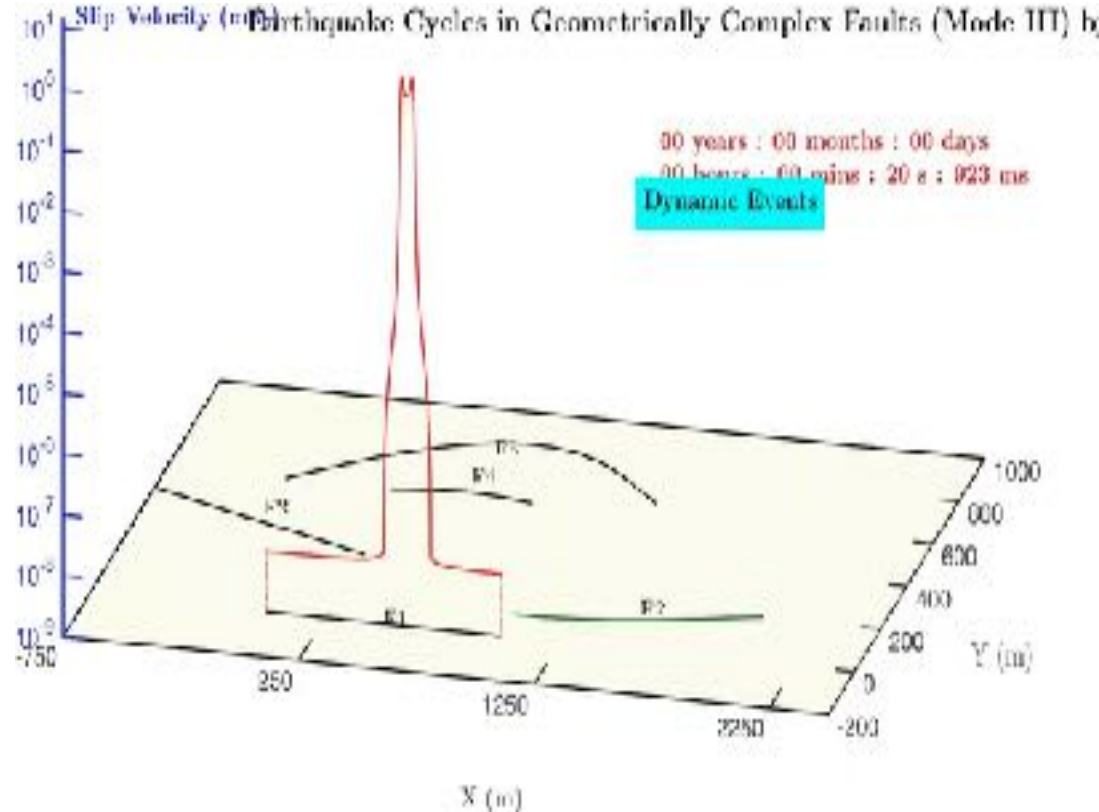
(*Barbot 2019b*)

Acceleration with Hierarchical-Matrix (FastCycles)

The quasi-dynamic boundary can be accelerated using hierarchical matrix (H-Matrix).

Large matrices are approximated by block-wise singular value decompositions.

Examples: Two-dimensional (plane strain) simulations of quasi-dynamic seismic cycles in a fault network (Pierre Romanet & Harsha Bhat, pers. comm.)



Authors/Developers: Pierre Romanet, Harsha S. Bhat

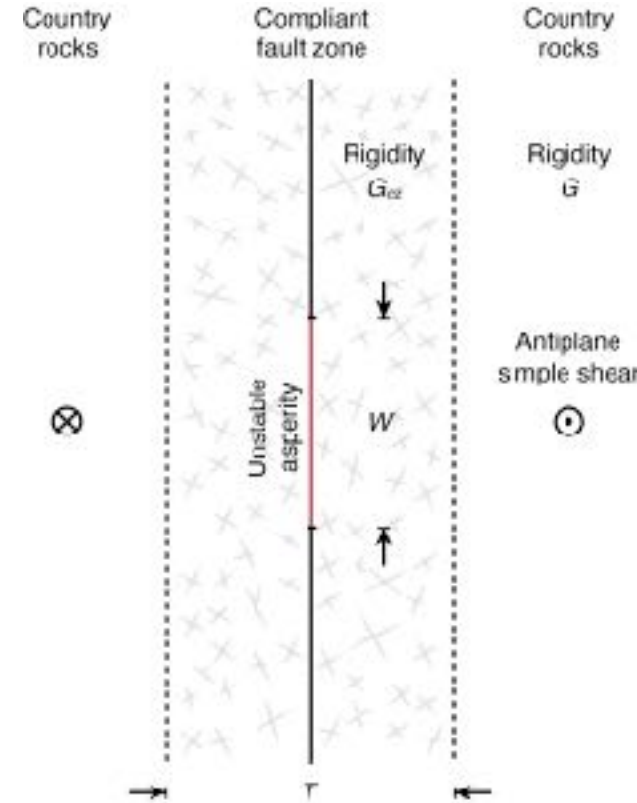
Method 4: Quasi-dynamic spectral boundary integral method (SBIM-qd)

Another flavor of the boundary integral method combines the quasi-dynamic approximation with the computational efficiency of the fast Fourier transform. For example, the stress interaction within a fault embedded in a compliant zone can be written (e.g., *Idini & Ampuero 2020*)

$$\tau(k) = -G_{cz}\pi k \coth\left[\pi T k + \operatorname{arctanh}\frac{G_{cz}}{G}\right](s - V_L t) - G_{cz}\frac{V}{2V_S}$$

Using the Fourier transform is applicable for planar, parallel faults and a layered elastic structure.

(Nie & Barbot 2022)

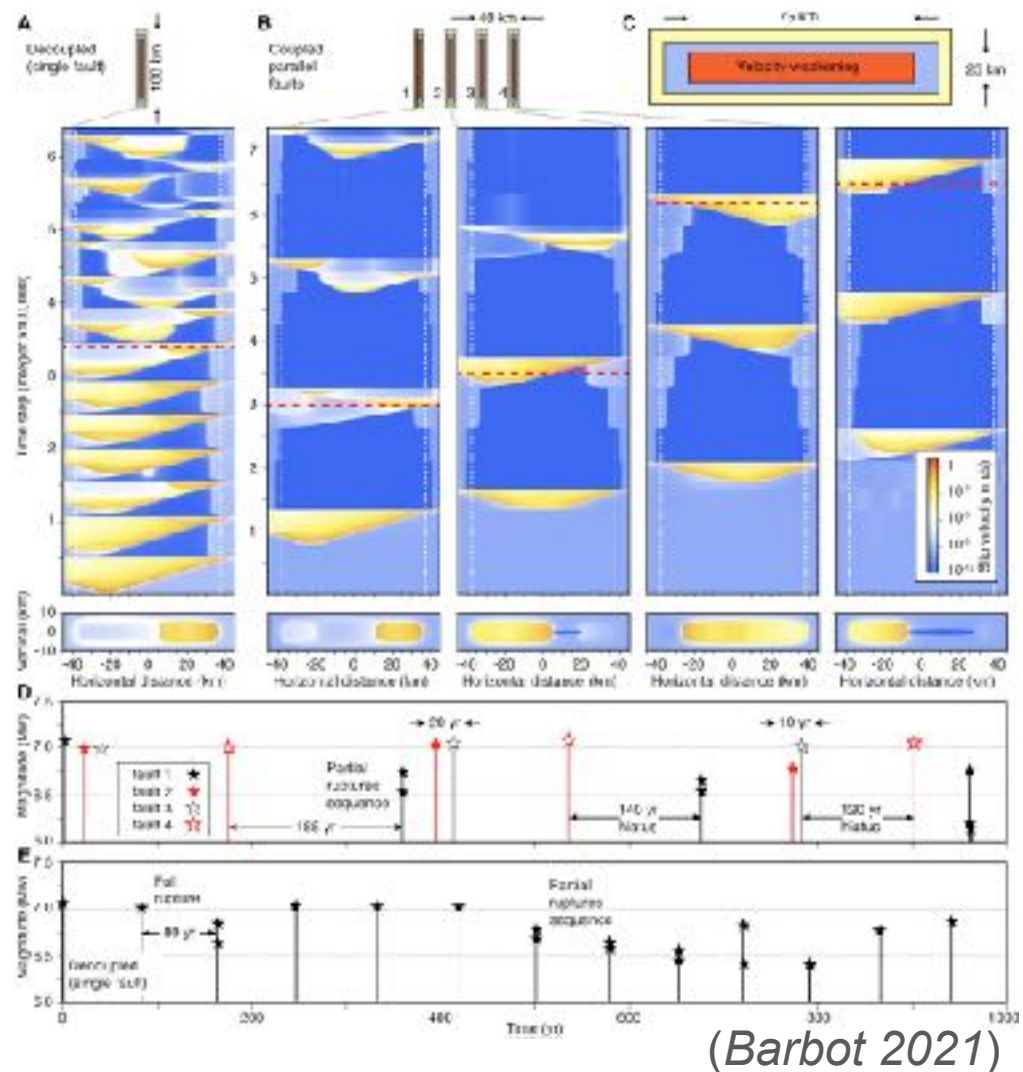


Applications of SBIM-qd with Motorcycle

Use numerical simulations to explore triggering of ruptures within a network of faults.

Example: Earthquake interactions in a fault network. Clustering of events in Southern California on the parallel Rose-Canyon-Inglewood-New Port, Elsinore, San Jacinto, and San Andreas faults (*Barbot, 2021*).

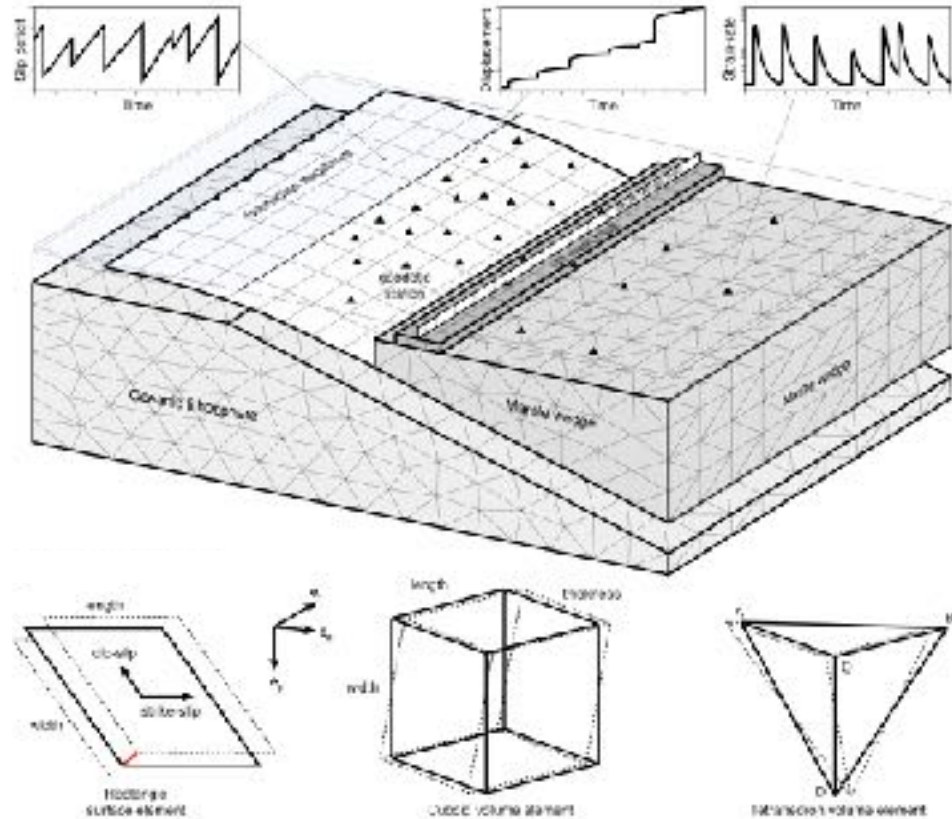
Motorcycle: <https://bitbucket.org/sbarbot/motorcycle/src/master/>



Method 5: Quasi-dynamic integral method (IM-qd)

The integral method combines surface elements (rectangles, triangles) and volume elements (e.g., cuboid, tetrahedra) to simulate the mechanical coupling between localized and distributed deformation.

The approach is useful to model seismic cycles in a viscoelastic or poroelastic medium with a nonlinear rheology, accounting for the free surface.

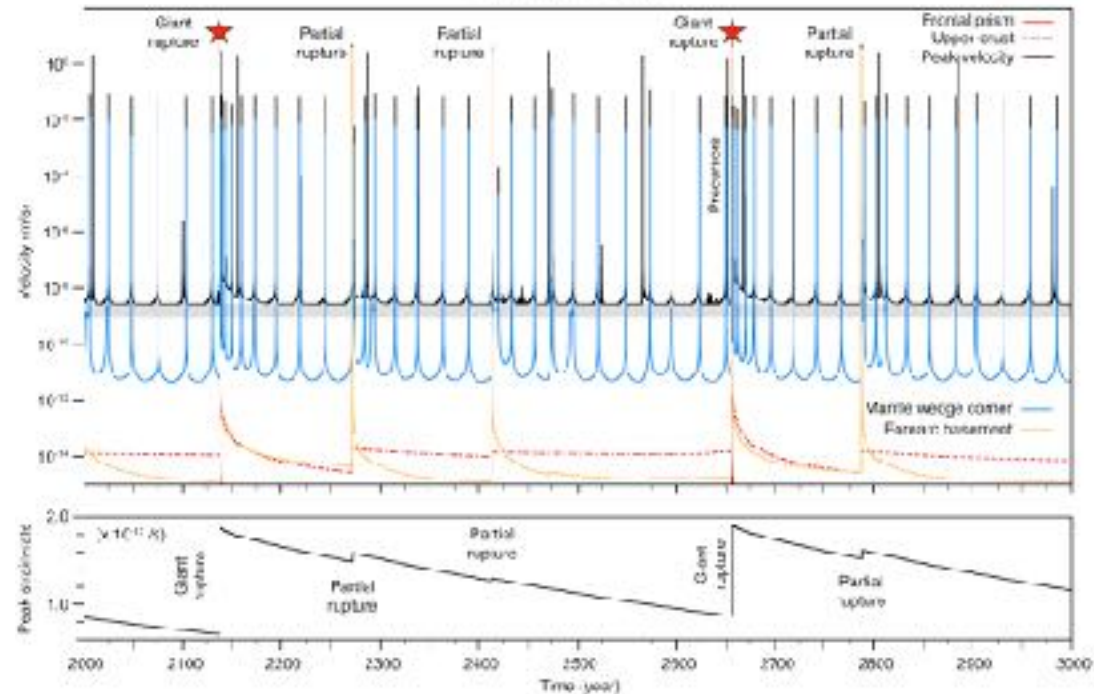
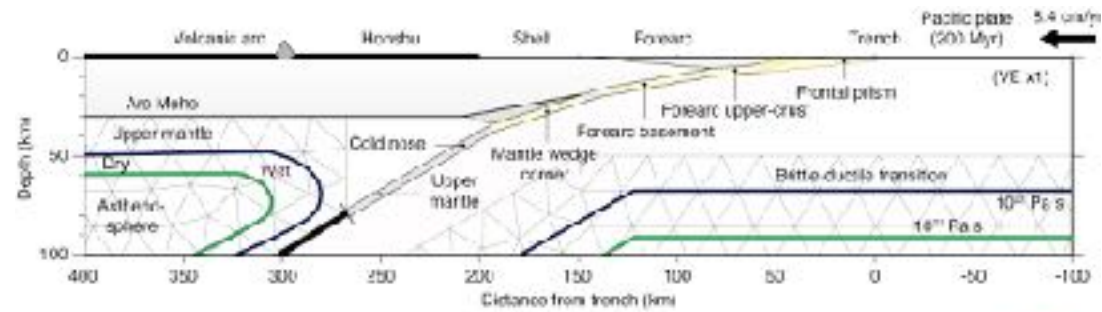


(Barbot, pers. comm. 2022)

Application of IM-qd with Unicycle

Integrated models of the lithosphere-asthenosphere system can be obtained with the integral method.

Example: Seismic super-cycles at the Japan Trench with viscoelastic relaxation following all large earthquakes. Models reproduce giant Mw 9.1 Tohoku earthquake co- and post-seismic deformation (*Barbot, 2020*).

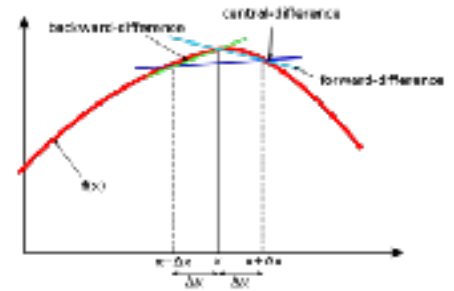


(*Barbot 2020*)

Method 6: Finite difference method

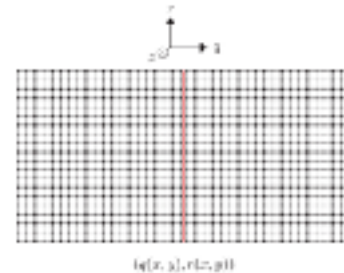
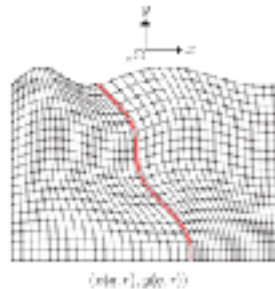
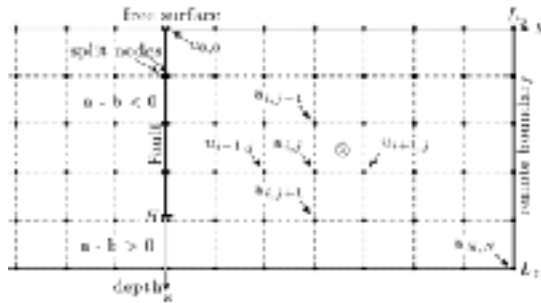
In general, the approximation of derivatives with difference equations

$$f'(x) = \frac{f(x + \Delta x) - f(x)}{\Delta x}$$



The domain is discretized into a structured grid of points, which may be collocated or staggered, and complex geometry can be handled with a curvilinear coordinate transform.

Domain discretization, (Erickson and Dunham 2014)



Curvilinear coordinate transform

To ensure conservation of energy, can use summation-by-parts (SBP) operators and weakly enforced boundary conditions (e.g. Mattson and Nordstrom, 2004; Erickson and Dunham, 2014)

Example: momentum balance equation

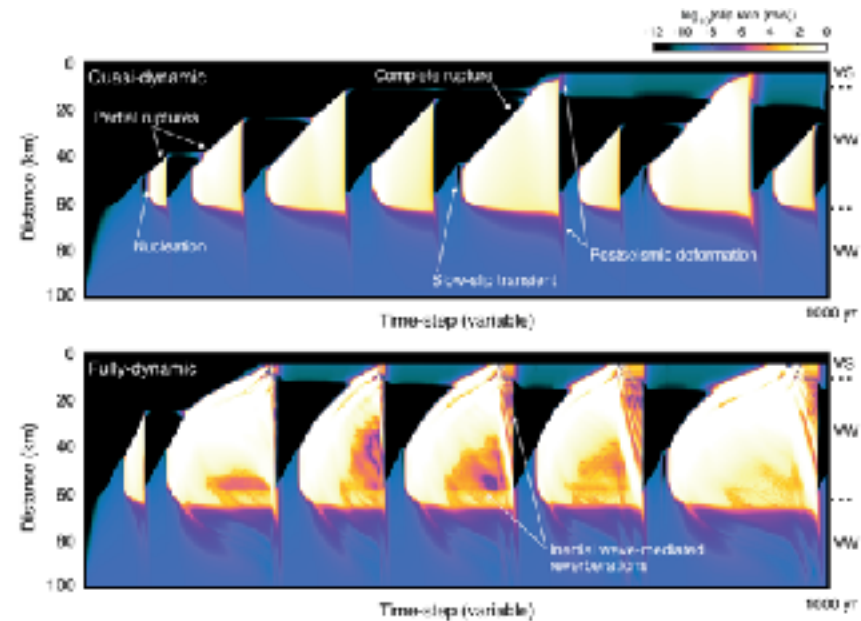
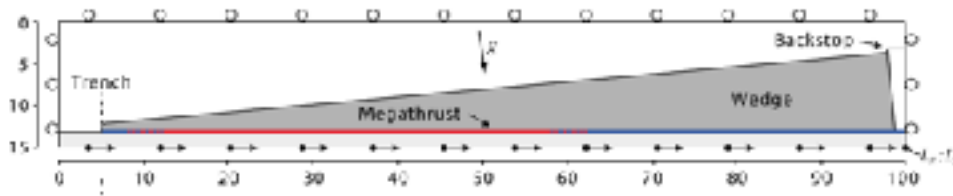
$$\rho \ddot{u} = \nabla \cdot (\mu \nabla u) \implies \rho \ddot{u} = D_{xx}^\mu u + p$$

D_{xx}^μ derivative matrix
 p boundary condition terms

Applications with Velo2cycles (Visco-elastic 2D cycles of earthquakes)

Two-dimensional continuum-based, finite difference model for fault slip and off-fault deformation in a visco-elasto-plastic rheology.

Simulation of in-plane and anti-plane strain problems and allows investigating quasi-dynamic and fully dynamic problems with multiple faults, a free surface, temperature-dependent (power-law) rheologies, and rate- and state-dependent friction in a domain with spatially varying properties.

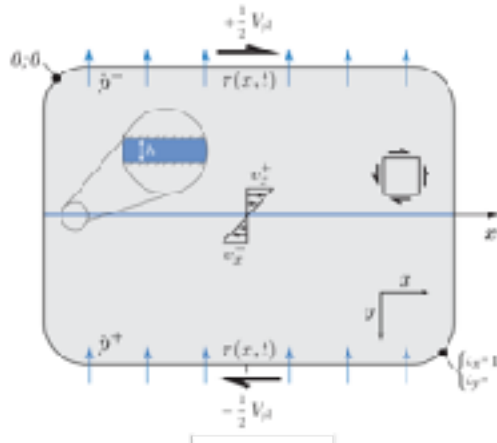


Wedge setup to test variable on-fault and off-fault properties.

Applications with H-MECs (Hydro-Mechanical Earthquake Cycles)

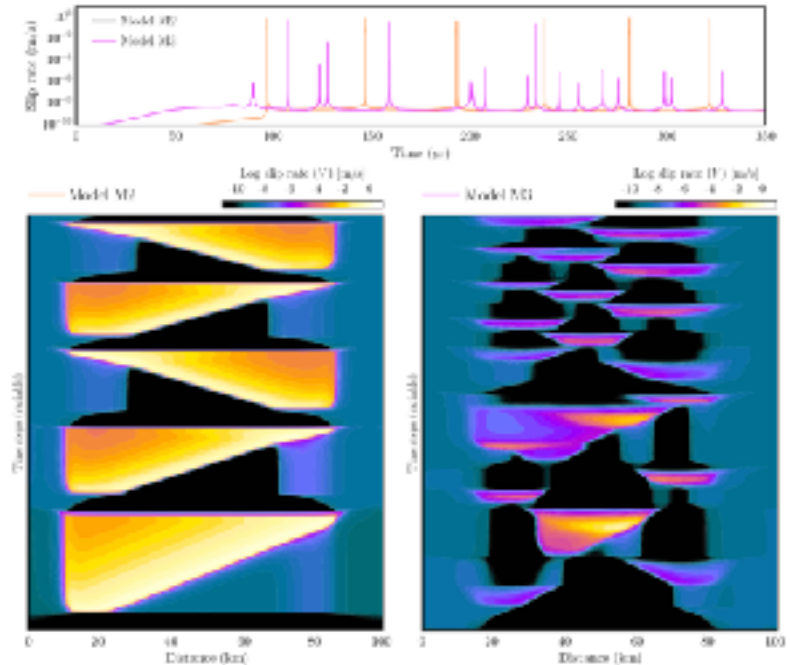
Two-dimensional, continuum-based finite difference code with a fully coupled (solid-fluid) formulation and fault slip governed by rate- and state-dependent friction.

This method accounts for fully dynamic wave-mediated effects, compressible poroelastic medium, and spatially varying mechanical and hydraulic properties.



Example of a simple 2-D, strike-slip setup with inflow/outflow boundary conditions, far-field loading, and a fault with a finite thickness

Results: Examples of fluid-driven sequences of seismic and aseismic slip with low (M2) and high (M3) pore-fluid pressure



Authors/Developers: Dal Zilio et al. (2022, *Tectonophysics*)

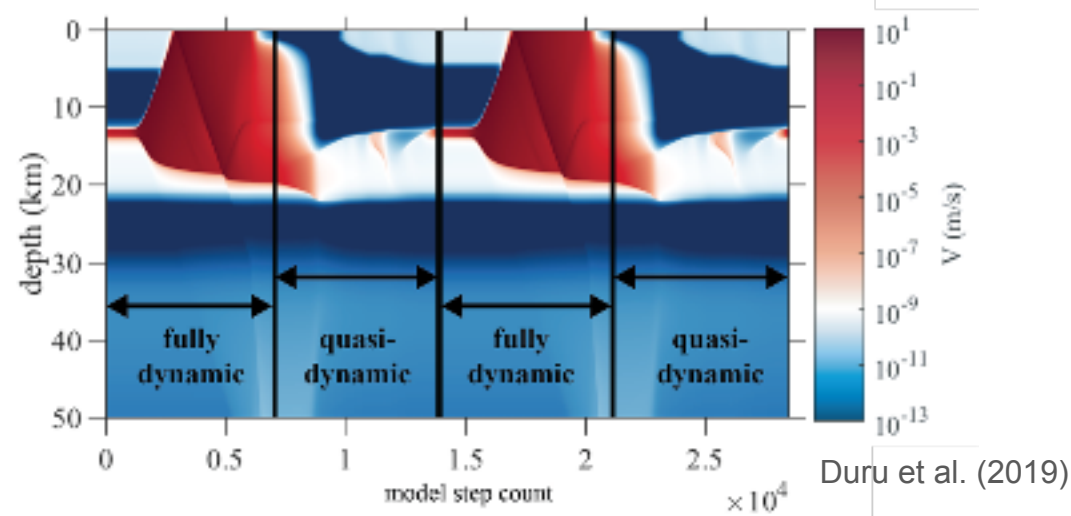
Applications with SCycle

Two-dimensional finite difference code for fault slip and off-fault deformation in a viscoelastic medium (*Duru et al. 2019*).

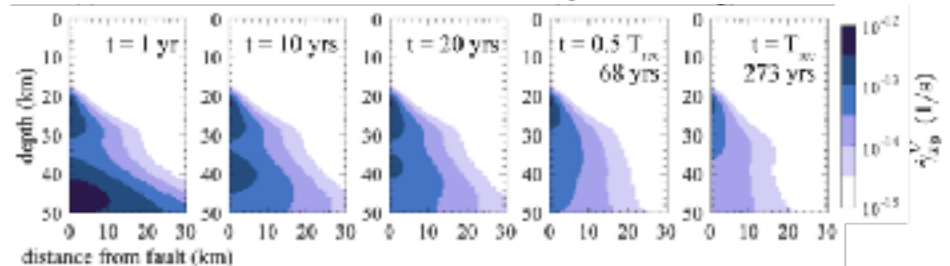
Solves anti-plane strain problems with a vertical strike-slip fault.

Includes both quasi-dynamic and fully dynamic formulations, a free surface, fluid flow along the fault, temperature-dependent and grain-size dependent (power-law) rheologies, with rate- and state-dependent friction in a domain with spatially varying properties.

Viscoelastic cycles with full inertia in the coseismic phase



Evolution of viscous strain rate during the interseismic period



Method 7: Continuous Galerkin finite element method (FEM-cg)

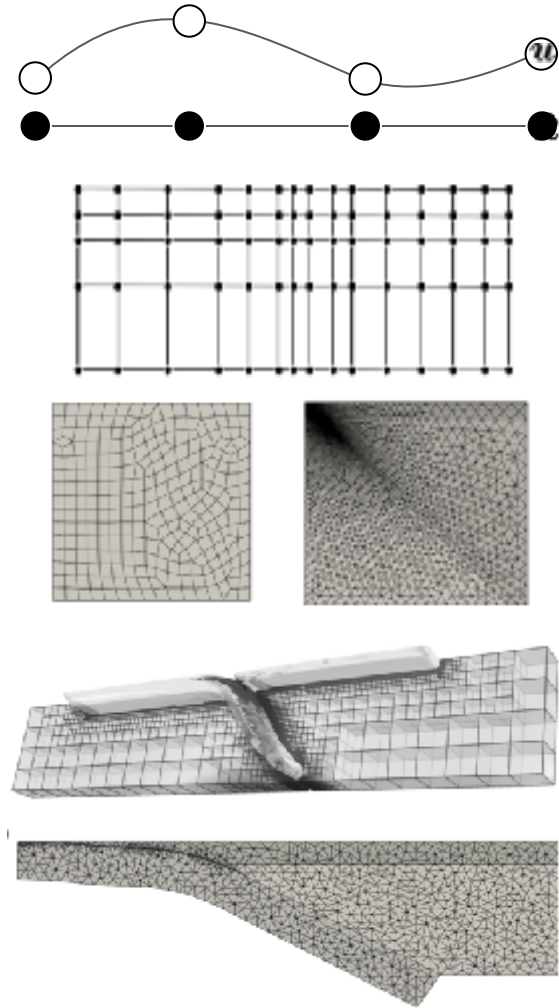
In the **continuous Galerkin** finite element method (FEM-CG), a discrete solution is associated with a weak formulation of the partial differential equation, defined as a polynomial over each element. The **continuity of the solution is explicitly imposed**.

As a method based on volume discretization, it offers versatility:

- Spatially variable material properties permitted.
- Geometrically flexible w.r.t. domain and fault.
- Algorithmically optimal and scalable solvers for QD problems exist.
- SEM highly accurate and efficient for fully dynamic problems.

Disadvantages: computational cost

- Expensive compared to finite difference (more degrees of freedom).
- Fault requires break in continuous function space (split nodes).
- Complex fault topology is non-trivial.



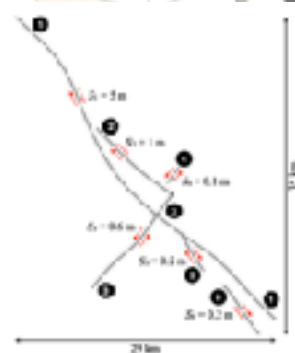
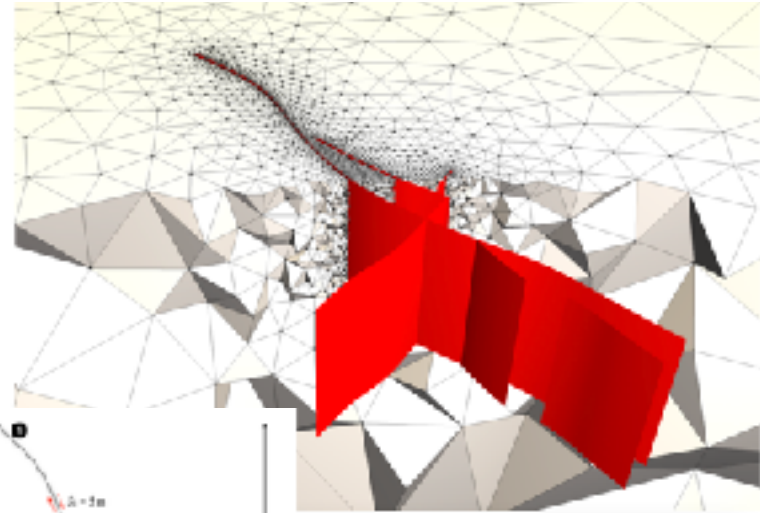
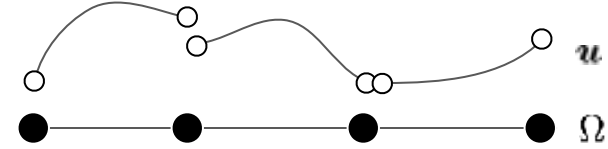
Method 8: Discontinuous Galerkin finite element methods (FEM-dg)

With the **discontinuous Galerkin** finite element method, the solution is allowed to be discontinuous across element boundaries.

The approach affords and even wider variety of mesh types that naturally accommodate faults. Complex fault topology becomes trivial. For example, intersecting and branching faults do not require special treatment.

Disadvantages of DG-FEM

- More expensive cf. CG FEM (even more DOFs than CG FEM)
- Dev. of scalable optimal solvers (QD problems) lags behind CG FEM



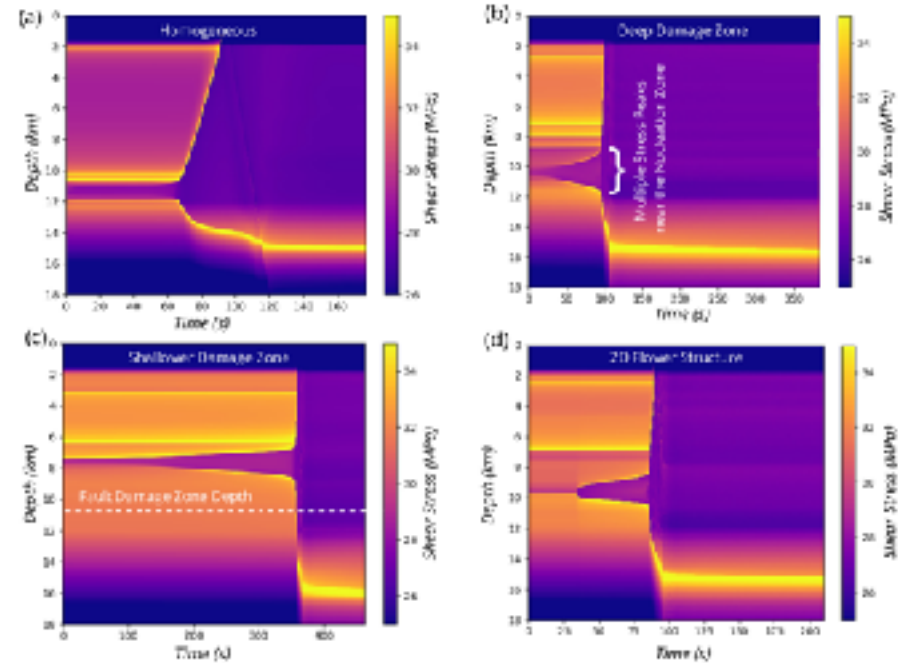
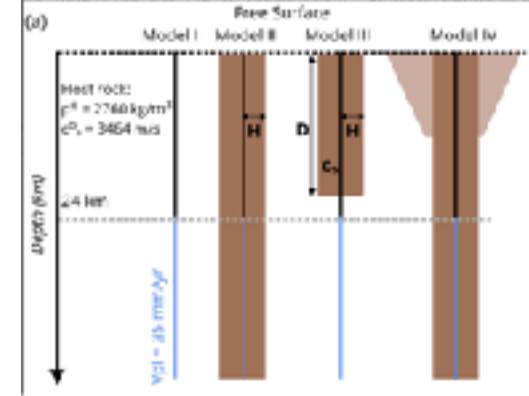
(DG-FEM, Rigdecree fault system, Uphoff et al., EarthArxiv '22)

FEM-cg applications with SPEAR

SPEAR is an open-source, fully dynamic spectral element method (SEM) using algebraic multigrid.

Example: Two-dimensional fully dynamic volumetric seismic cycle simulation on a strike-slip fault surrounded by a low-velocity damage zone (Thakur et al., 2020, JGR)

SPEAR: <https://github.com/thehalfspace/Spear>

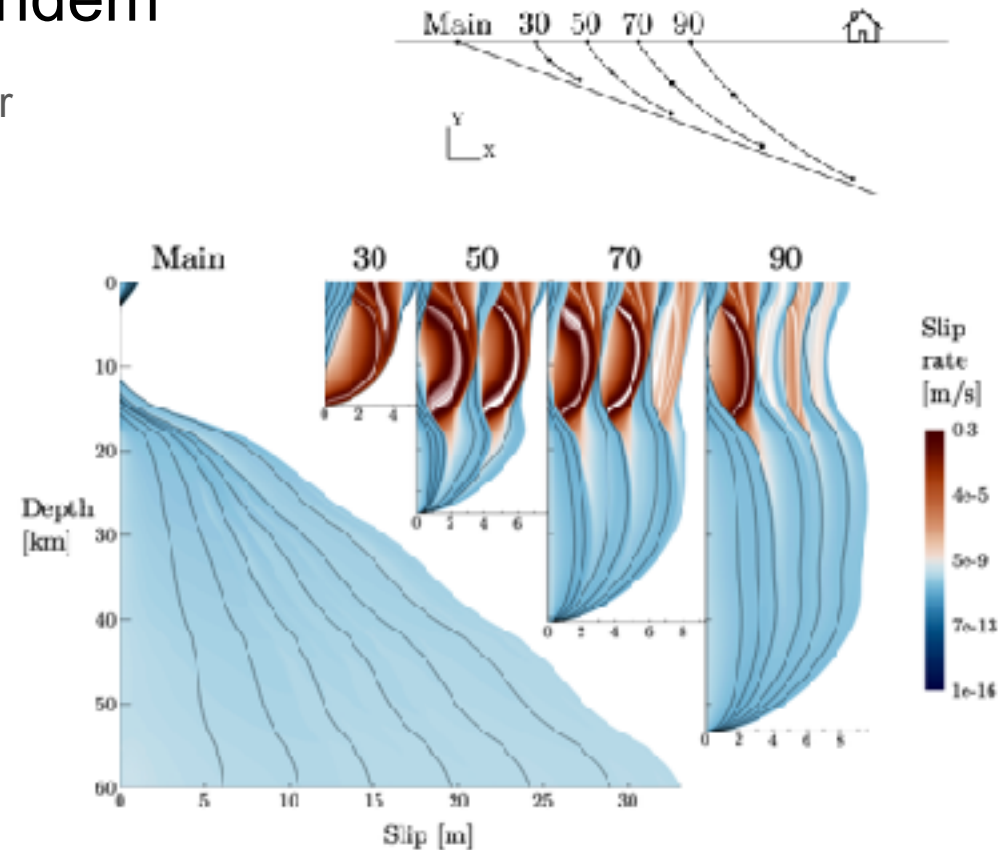


FEM-dg applications with Tandem

Tandem is an open-source symmetric interior penalty Galerkin (SIPG) code using PETSc, tested on up to 5000 MPI ranks. It allows for 2D and 3D multiple faults (non intersecting, branching, or intersecting), curvilinear meshes, optional discrete GFs and spatially varying elastic properties.

Example: 2D quasi-dynamic cycles of multiple splay faults interacting with a shallowly dipping main fault, run-time (120 ranks, 0.5 km on-fault resolution) Green's functions 1.1 day, time integration 0.9 day (Uphoff et al. 2022, EarthArxiv).

Tandem: <https://github.com/TEAR-ERC/tandem>

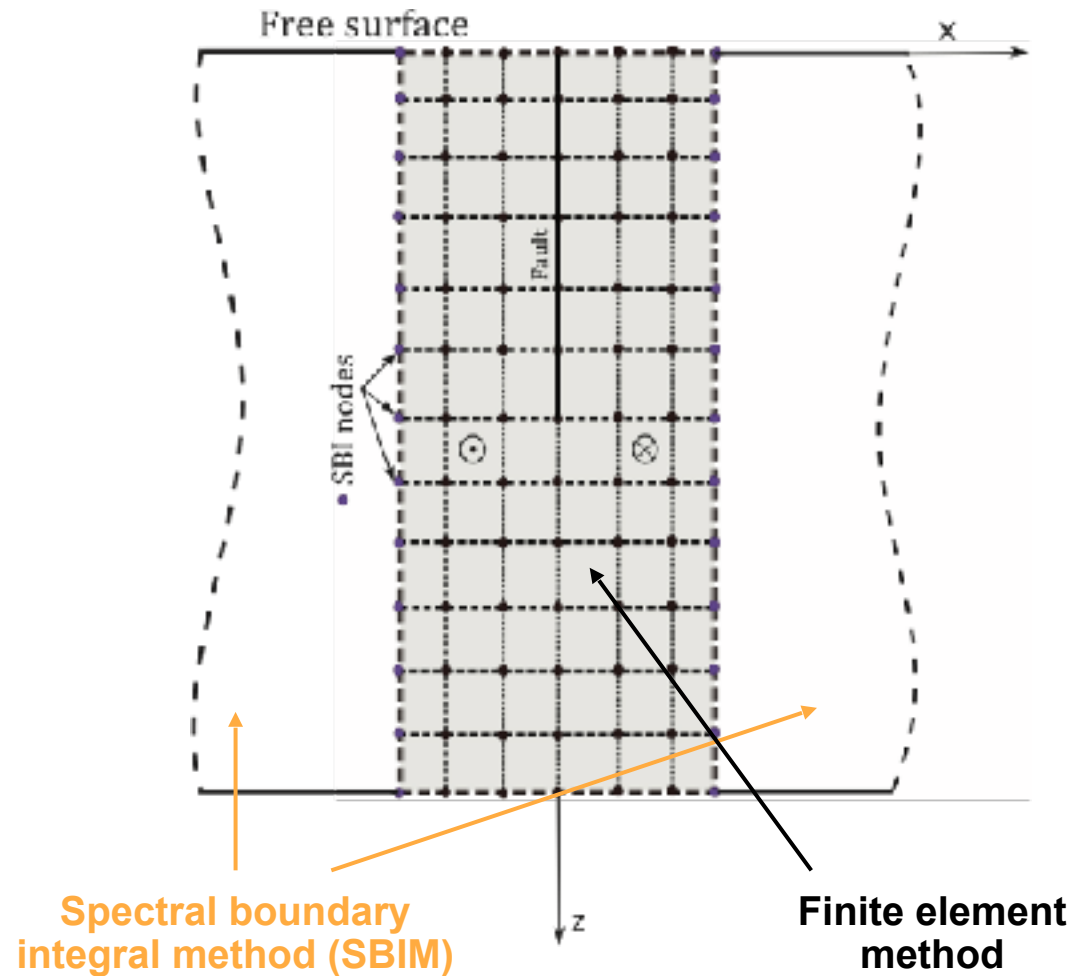


(Uphoff et al. 2022, EarthArxiv)

Hybrid methods

Various methods can be combined to maximize versatility and computation efficiency.

Example: Combination of the finite element method and spectral boundary elements to simulation fully dynamic seismic cycles on a fault embedded in a compliant zone (*Abdelmeguid et al. 2019*).



(*Abdelmeguid et al. 2019*)

Current modeling capabilities for seismic cycle simulations

	Fully dynamic space-time boundary integral method (BIM-fd)	Spectral boundary integral method (SBIM)	Quasi-dynamic boundary integral method (BIM-qd)	Volumetric method (FD, FEM, DG)
Dimension	2D/3D	2D/3D	2D/3D	2D/3D
Inertia	Yes	Yes	Radiation damping	Yes
Fault morphology	Planar, non-planar, multiple faults	Planar fault	Fault network	Planar, non-planar, multiple faults
Distributed deformation	Limited	Limited	Viscoelastic	Viscoplastic
Material heterogeneity	Limited	Limited	Limited	Fine-grain
Fault evolution	No	No	No	Allowed
Computational cost	High	Low	Intermediate	Very high
Publicly available code	No	Very few	Some	Some

Open source software for seismic cycle modeling

- <https://github.com/ydluo/qdyn> (BIM-qd)
- <https://bitbucket.org/sbarbot/motorcycle/src/master/> (SBIM-qd)
- <https://github.com/geodynamics/pylith> (FEM)
- <https://github.com/sozawa94/hbi> (BIM)
- <https://github.com/tbenthompson/tectosaur> (BEM)
- <https://gitlab.com/uguca/uguca> (SBIM)
- <https://pangea.stanford.edu/~edunham/codes/codes.html> (SBIM)
- <https://bitbucket.org/kallison/scycle/src/master/> (FD, viscoelastic)
- <https://github.com/TEAR-ERC/tandem> (DG-FEM, curvilinear grids)
- <https://bitbucket.org/cpranger/garnet> (FD, viscoelastic)
- <https://github.com/thehalfspace/Spear> (CG-FEM)
- <https://github.com/brittany-erickson/FDCycle> (FD)

Discussion

Spatial resolution requirements

Estimates of the size of nucleation of frictional instabilities for finite faults (Noda & Hori 2014) depend on the ratio of frictional parameters a/b . For $a/b > 0.5$,

$$h^* = \frac{\pi}{4} \frac{GbL}{(b-a)^2 \bar{\sigma}}$$

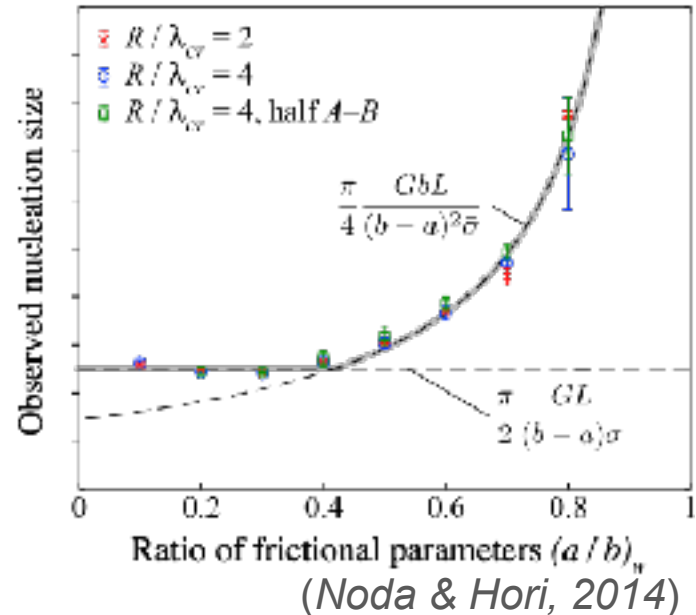
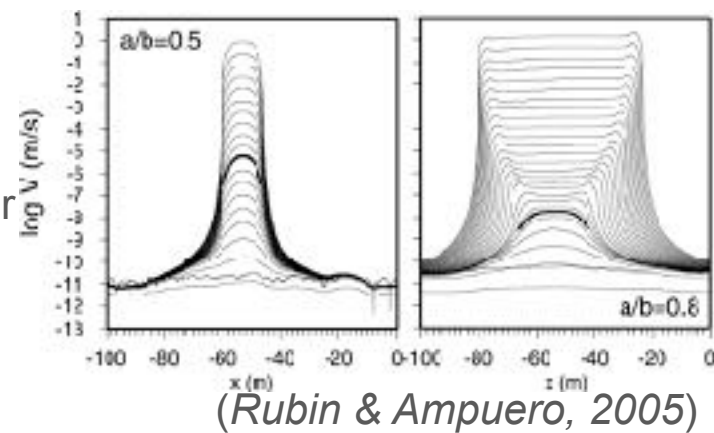
For $a/b < 0.5$,

$$h^* = \frac{\pi}{2} \frac{GL}{(b-a)\bar{\sigma}}$$

In addition, strong gradients of stress near the rupture front can be characterized by a cohesive length (Day et al. 2005, Ampuero & Rubin 2008)

$$\Lambda \propto \frac{GL}{b\bar{\sigma}}$$

The shortest of these length scales must be sampled finely.



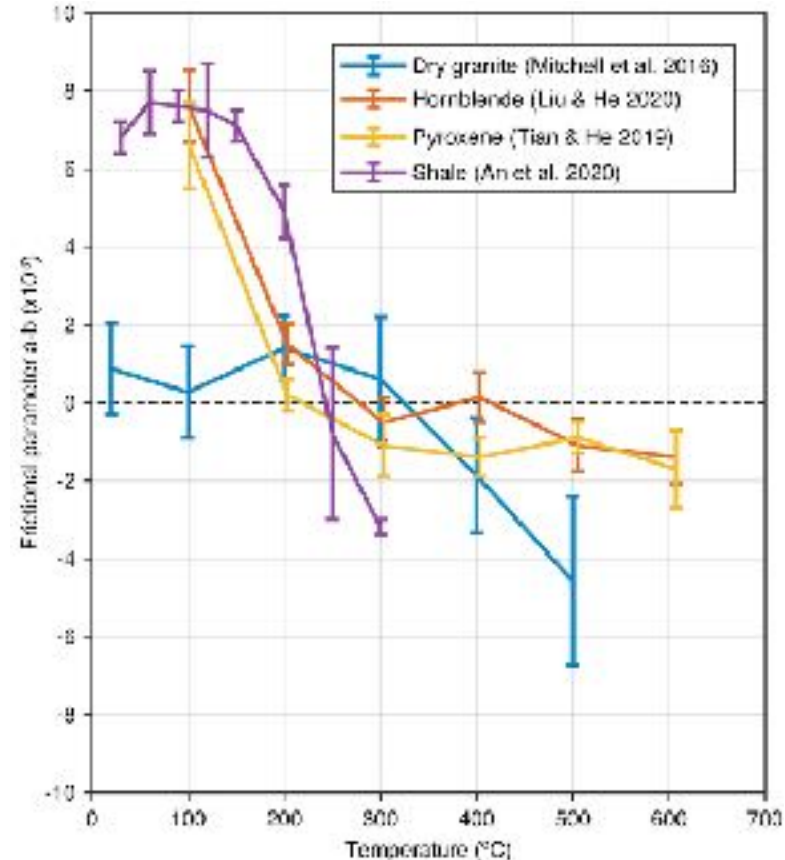
Constraints on frictional parameters

Frictional parameters are typically constrained from laboratory experiments. For example, **granite** (Stesky 1978, Lockner et al. 1986, Blanpied et al. 1991, 1995, Chester 1995, Mitchell et al. 2016), **olivine** (Boettcher et al. 2007), **pyroxene** (Tian & He 2019), **hornblende** (Liu & He 2020), **serpentinite** (Okuda et al. 2021), **shale** (An et al. 2020), SAFOD **gouge** (Moore et al. 2016), Alpine Fault (Boulton et al. 2014), Longitudinal Valley Fault (den Hartog et al. 2021), **phyllosilicates** (collettini et al. 2019), **carbonates** (Chen et al. 2015), and many others.

Other constraints are obtained from modeling seismo-geodetic observations (e.g., Lindsey and Fialko 2016, Thomas et al. 2017).

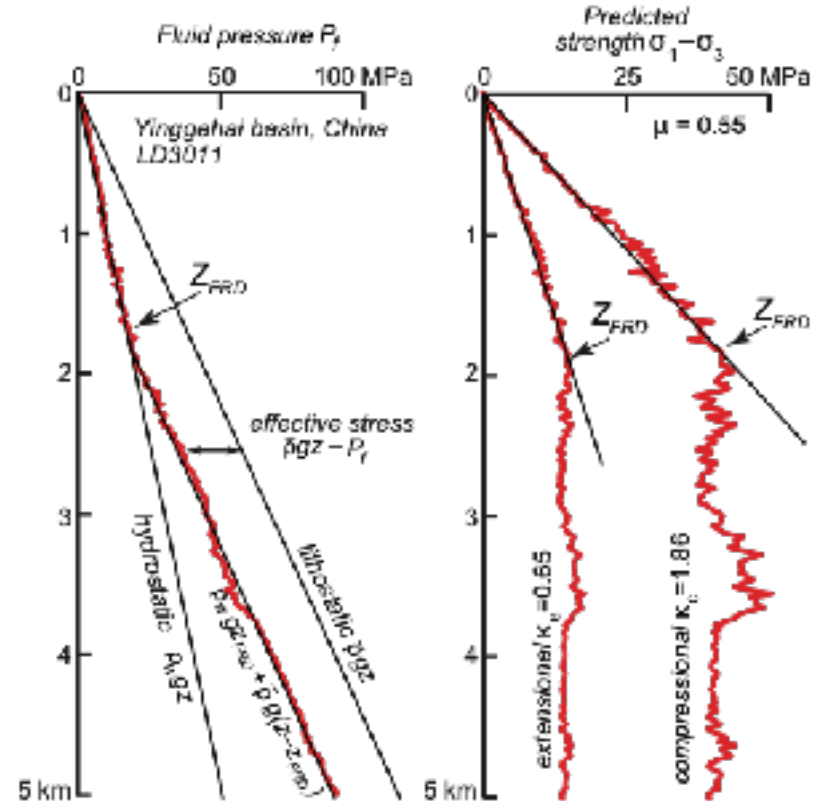
However, the frictional properties of rocks are complex and poorly understood, depending at least on **mineralogy**, **temperature**, **velocity**, **normal stress**, and **water content**.

Additional mechanisms, such as thermal pressurization and flash weakening require additional physical properties.



How to choose effective normal stress distribution

- Lithostatic pressure minus hydrostatic pore pressure (*Sibson, 1974*)
- Assume high fluid over-pressurization at depth
- Hydrostatic pore pressure gradient at shallow depths, transition to lithostatic pore pressure gradient with constant offset at depth (e.g. *Lapusta et al., 2000*)
- Simulate pore fluid pressure evolution (e.g., *Noda and Lapusta 2013; Zhu et al. 2020*)



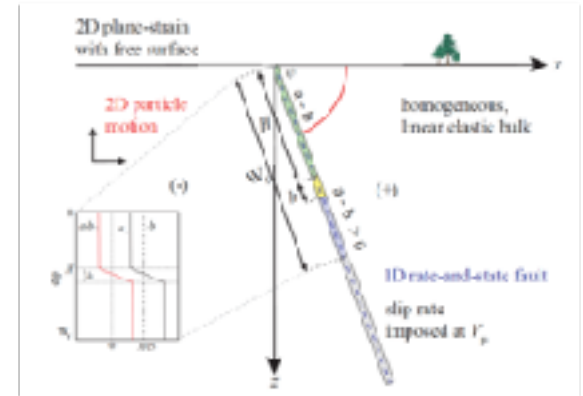
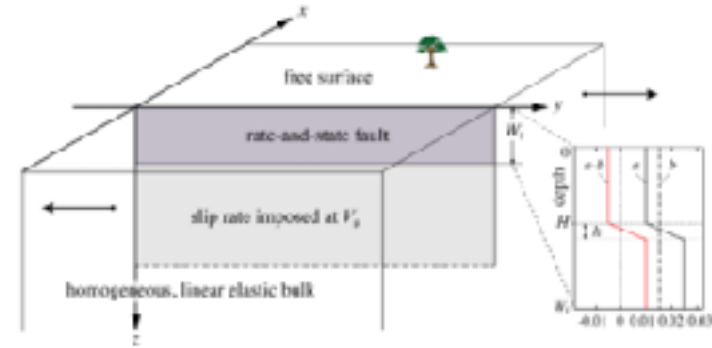
Loading the mechanical system

Loading of a fault system is essential to attain seismic cycles.

- Long-term fault slip-rate
- Background rate of stress
- Displacement of remote boundary

The volume-discretization method affords better flexibility for loading, especially for complex structural settings (multiple faults, free surface, heterogeneous loading from all sides).

A desirable goal is to link seismic cycles to long-term geodynamics models that dictate the location and geometry of faults and the overall loading rate from all sides (e.g., Sathiakumar et al. 2020).



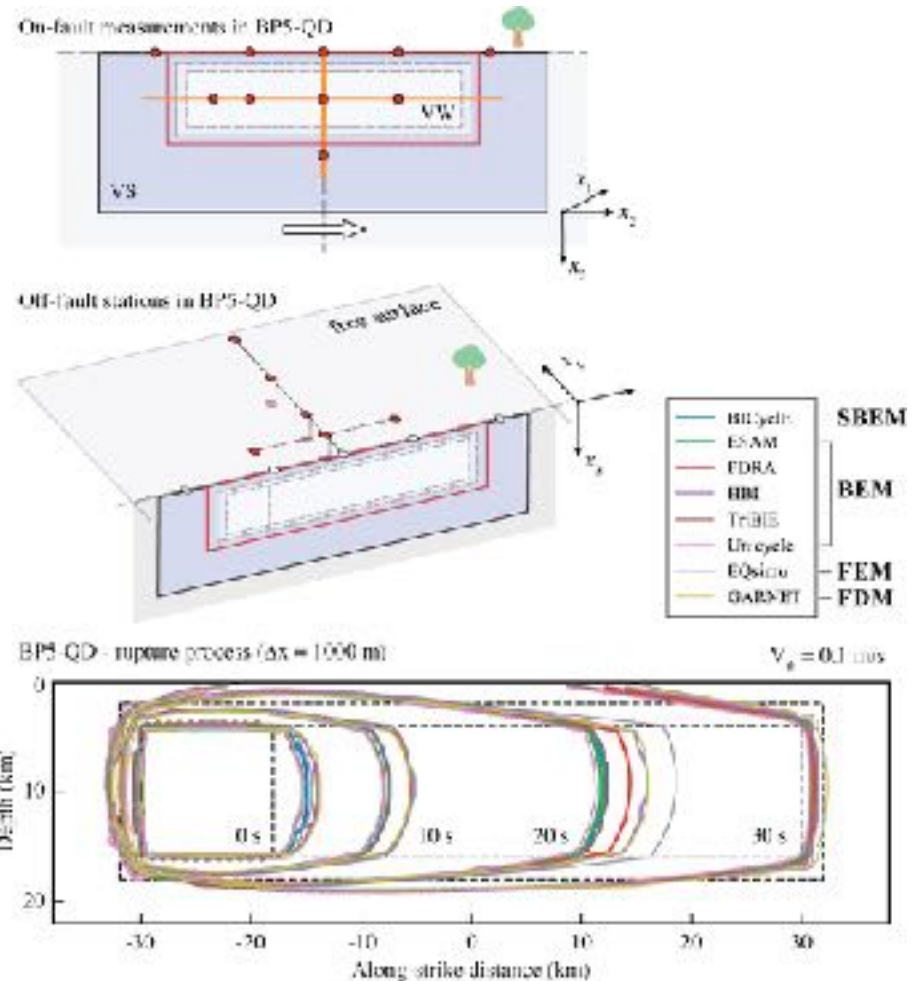
Figures from SCEC SEAS benchmarks BP1-QD and BP3

Benchmarks

Detailed problem specification - from initial and boundary conditions to material properties - allows comparison of numerical solutions based on different computational methods.

The SCEC Sequence of Earthquakes and Aseismic Slip (SEAS) project has produced 7 such benchmarks (*Erickson et al. 2020, Jiang et al. 2022*). <https://strike.scec.org/cvws/cgi-bin/seas.cgi>

Additional benchmarks are required for a wide range of problems, including for subduction zones and oceanic transforms.



(*Jiang et al. 2022*)

Conclusions

Multiple numerical methods are available to simulate seismic cycles, including with **internal boundary** and/or **volume discretization**.

The degree of simplification of the problem dictates the most efficient method, with the spectral boundary-integral method (SBIM) being the fastest to simulate a single planar fault in an elastic full space, and volume methods being the most versatile.

Numerical simulations must resolve the finest length scale of the problem, which oftentimes is the cohesion length of the rupture front. However, other fine length scales appear with added physics (e.g., shear heating and off-fault diffusion). The time scales of dynamic rupture and fault healing being so widely different, adaptive time stepping is a must.

The seismic cycle working group will guide developers as they make open-source software available to the community while keeping full ownership of their own code.



Seismic cycle modeling online symposium

Programme (by chronological order)

- Nadia Lapusta, “Importance of inertial and poroelastic effects for simulations of sequences of earthquakes and aseismic slip (SEAS)”
- Luca Dal Zilio, “Earthquake sequence simulations with fault zone fluid flow, pore pressure evolution, and viscoelasticity”
- Eric Dunham, “The role of compaction, dilatancy, and permeability evolution in modulating pore pressure and fault slip”
- Kali Allison, “Interaction between earthquakes and viscoelastic interseismic deformation”
- Sylvain Barbot, “Numerical simulations of seismic cycles in a viscoelastic half-space with the integral method”
- Michelle Almakari, “Understanding the effect of injection protocol on induced seismicity: Insights from numerical experiments”
- Brittany Erickson, “A non-stiff, high-order accurate finite difference method for fully-dynamic earthquake sequence simulations within sedimentary basins”
- Ahmed Elbanna, “Modeling sequence of earthquakes and aseismic slip with high resolution fault zone physics”
- Esteban Rougier, “Using the combined finite-discrete element method to capture coseismic off fault damage”
- Yihe Huang, “Fully dynamic earthquake cycle simulations with fault damage zones”
- Sharadha Sathiakumar, “Impact of faulting and folding on earthquake cycles in collisional orogens”
- Pierre Romanet, “Effect of fault geometry on earthquake cycle using the spectral boundary element method”
- Yajing Liu, “Modeling earthquake and slow slip sequences with three-dimensional fault geometry”
- Stéphanie Chaillat, “An overview of the capabilities of fast Boundary Element Methods for wave propagation problems”
- Ryosuke Ando, “Accelerating quasi-dynamic and dynamic boundary element simulations by hierarchy matrices”
- Dave May, “A symmetric interior penalty discontinuous Galerkin method for seismic cycling”
- Luc Lavier, “Modeling the seismic cycle within a fault zone of finite thickness”
- Alice Gabriel, “Volumetric seismic cycle modeling using tandem: fault geometry and multi-fault interaction”
- Benchun Duan, “An explicit finite element dynamic earthquake simulator for slip behaviors of subduction zones and geometrically complex faults”
- Casper Pranger, “The hidden dimension in fault simulations: insights from a new internal rate and state friction rheology with an interaction length scale”
- Makiko Ohtani, “Numerical experiments on estimation of the frictional properties and slip evolution on the Bungo SSE fault with adjoint method”